



Liquefaction susceptibility and re-liquefaction potential of the liquefied soil site caused due to M_w 5.7 Tripura earthquake

KUNJARI MOG^{1,*} and P ANBAZHAGAN²

¹Department of Civil Engineering, National Institute of Technology Hamirpur, Hamirpur, Himachal Pradesh 177005, India

²Department of Civil Engineering, Indian Institute of Science, Bangalore, Karnataka 560012, India
e-mail: kunjari@nith.ac.in; mogkunjari@gmail.com; anbazhagan@iisc.ac.in

MS received 2 February 2024; revised 20 June 2024; accepted 23 August 2024

Abstract. On January 3, 2017, an earthquake measuring M_w 5.7 struck 19 km east of Ambassa in Tripura, India, leading to soil liquefaction, lateral spreading, and landslides in the epicentral area. This paper presents the results of comprehensive field investigations of liquefied soil sites following the 2017 Tripura earthquake. The study involved conducting Standard Penetration Test (SPT) and Multichannel Analysis of Surface Wave (MASW) tests to evaluate the penetration resistance and shear wave velocity (V_s) profile of the sites. These data were subsequently utilized to determine the liquefaction potential index (LPI). Results from the field tests revealed low SPT N, low V_s , and high LPI values at shallow depth, indicating the presence of thick and loose soil layers at the site. This study is particularly valuable to the earthquake engineering community, as there are limited available case histories documenting in-situ soil properties at liquefaction sites triggered by earthquakes below magnitude 6.

Keywords. Tripura earthquake; liquefaction and re-liquefaction; multichannel analysis of surface wave (MASW); standard penetration test (SPT); liquefaction potential index (LPI); moment magnitude.

1. Introduction

The study of liquefaction phenomenon in soil dynamics has garnered extensive attention due to its potential to cause earth settlement, ruptures, and loss of life during and after earthquakes. Significant advancements in understanding liquefaction were made following the devastating effects of the Niigata earthquake in Japan and the Alaskan earthquake in the USA in 1964 [1]. Despite these advancements, liquefaction-related damages continue to be a prominent cause of destruction worldwide, as evidenced by earthquakes like Bhuj earthquake in India in 2001, New Zealand earthquake in 2011, Nepal earthquake in 2015 [2–4], and numerous other locations. Hence, it becomes imperative to accurately map or predict liquefiable layers in earthquake-prone areas. Such information is essential for guiding future structure design, implementing retrofitting measures, and conducting seismic hazard assessments.

Numerous studies conducted worldwide have focused on developing methodologies for liquefaction analysis of soils, utilizing both penetration-based approaches (e.g., SPT, CPT, Becker Penetration Test) and surface wave velocity (SWV) methods. Among these methods, Seed and Idris's SPT-based approach, commonly known as the “simplified

procedure,” has gained widespread adoption and become a standard practice in several countries since its inception in 1971 [5]. Over the years, this “simplified procedure” has undergone multiple revisions and updates [6–8]. However, the reliability of SPT measurements obtained from hard strata or gravelly soils is highly questionable, necessitating a complementary approach to penetration-based methods. Likewise, CPT-based methods, exemplified by Robertson and Wride's “CPT-based simplified procedure (1998)”, have also gained popularity [9]. Within this context, the in-situ shear wave velocity (V_s) measurement offers a promising alternative as it is a non-invasive technique [10–14]. Despite its potential, the database of V_s method based on field observations of liquefied sites during earthquakes of magnitude less than 6 remains scarce in the existing literature.

The 2017 Tripura earthquake, with a magnitude of M_w 5.7 and a focal depth of 31 ± 6.0 km, had its epicenter located 19 km from Ambassa and approximately 100 km from the capital city Agartala. This seismic event caused significant damage to buildings, with 5200 dwellings partially damaged, 1450 houses severely damaged, one fatality, and more than seven injured [15]. The earthquake induced liquefaction, lateral spreading, and slope failures at the Kanchanbari site near the Manu Riverbank, along with a landslide that blocked a 5 km road and affected local

*For correspondence

transit. Remarkably, this moderate magnitude earthquake represents the first recorded field liquefaction evidence in India for an earthquake of such magnitude (M_w 5.7). In the available case history database, there are relatively few instances documenting the in-situ soil properties at liquefaction sites triggered by earthquakes with a magnitude less than 6.0. The lowest magnitude that has caused liquefaction is documented as a magnitude of 5.0 during the mainshock event [16]. Thus, the data and observations from liquefiable soil deposits associated with earthquakes of magnitude 5.7 or smaller are particularly valuable for understanding and analyzing such events.

The present study focused on conducting in-situ investigations using SWV and SPT tests to analyze the liquefaction caused by the 2017 Tripura earthquake, India. Post-liquefaction field investigations were conducted, involving SPT to measure the site's penetration resistance and retrieval of soil samples from various depths. The soil samples obtained from SPT were then tested in the laboratory to determine index properties and bedding features. In addition, MASW (multichannel analysis of surface wave) tests were performed to establish the shear wave velocity profile at both the liquefied site and non-liquefied locations. The Liquefaction Potential Index (LPI) was also established for the first time in the region, to predict potential manifestations of liquefaction features at the ground surface. These investigations aim to provide valuable insights into liquefaction behavior and contribute to better seismic hazard assessments and future mitigation strategies.

2. Study area

The study area, Tripura, is situated in the northeastern part of India, close to the Himalayan belt. The state shares its borders with Mizoram to the east, Assam to the northeast, and Bangladesh to the west, south, and north. Tripura's geology comprises young sedimentary rocks of marine-mixed fluvial origin, which are approximately 38 million years old [17]. Due to its location at the convergent boundary of the Indian plate with the Eurasian plate, which moves at a rate of approximately 4.5 cm per year, the state is considered seismically vulnerable and falls under seismic zone V as per the Indian seismic code, with an anticipated zero period acceleration of 0.36 g [18].

During the 2017 Tripura earthquake, seismic intensities of V and VI were reported near the epicenter and the northeast side of the state. Figure 1 presents raw photographs of the liquefaction, while figure 2 shows a schematic diagram of the liquefied area (24.118° N and longitude 91.991° E). The surface manifestation of liquefaction appeared as linear sand boils, located approximately 11 km away from the epicenter, with greyish-colored sand deposits. The extent of liquefaction was not substantial but

covered an area of 290 m × 210 m, with linear sand boils (a), (b), (c), (d), and (e) having lengths of 114, 25.5, 32.3, 33.6, and 31 m, respectively. The thickness of the oozed-out soil deposits was measured to be around 15 to 30 cm.

At the liquefaction site, the surface peak ground acceleration (PGA) ranged from 0.152 g to 0.28 g [15]. Figure 3 shows the site locations of the present study area along with the SPT and MASW test locations. It is worth noting that about five to six decades ago, the Manu River used to run through the same area where the surface manifestation of liquefaction took place on January 3, 2017, during the Tripura earthquake, as depicted in the schematic diagram in figure 2. Over time, the riverbed gradually filled with flood deposits, forming a weak zone running parallel to the riverbed. As a result, during the shaking, this situation may have allowed for the development of linear liquefaction features along the weak zone parallel to the riverbed.

3. Materials and methodology

3.1 In-situ investigations

After the earthquake event, the authors collected ejected liquefied soil deposits from the site and transported them to the laboratory for further investigation. In addition, field SPT and MASW tests were conducted both at the liquefied location and around non-liquefied locations. Two SPT boreholes were drilled at the liquefied site (indicated by star symbols in figure 2) to investigate the soil properties, and two borehole data were collected from non-liquefied locations, as shown in figure 3. Five sets of seismic surface wave tests (MASW) were performed at the liquefaction location (marked by dashed lines in figure 2), and two sets of tests were performed at non-liquefied locations (represented by blue rectangular symbols in figure 3). In figure 3, the first, labeled as 1 and 2, represents the liquefaction site at Kanchanbari, Tripura. At this site, boreholes 1 and 2 were drilled, and five MASW tests were conducted. The second set of locations, labeled as 3 and 4, correspond to the testing sites (MASW and SPT) situated in areas unaffected by liquefaction.

3.2 Multichannel analysis of surface wave (MASW) test

The MASW test was employed to measure the shear wave velocity in the in-situ environment at the liquefied site. The MASW test relies on the Rayleigh wave, which is measured by a set of geophones placed on the ground surface. It generates a dispersion curve (Rayleigh wave velocity versus loading frequency) corresponding to varying wavelengths and determines the most probable soil profile. The MASW test can be conducted in two ways: the active and passive methods. In the present study, the active method



Figure 1. Surface manifestation of liquefaction as linear sand boils observed at the Kanchanbari, Tripura, India due to the 2017 Tripura earthquake.

was adopted to obtain a shallow depth profile. For the active method, a vibration source like a falling weight or mechanical vibrator is used to generate Rayleigh waves of shorter wavelengths, measuring wave properties at shallower depths.

At the liquefaction site, the MASW test was performed using 24 geophones placed in a straight line at equal intervals of 1 m spacing. Each geophone, acting as a vibration receiver with a minimum frequency of 4.5 Hz, was connected to a multichannel recorder and data

acquisition system. A 7.0 kg sledgehammer was used to create surface waves on the ground surface by hitting a 25 mm thick metal plate measuring 300 mm by 300 mm. These surface waves traveling between the geophones were recorded and processed. The recorded data was processed using the SurfSeis program, and the shear wave velocity profile was generated from the dispersion curve analysis. The outcomes of the MASW test from the liquefied site and non-liquefied sites are presented in the results section.

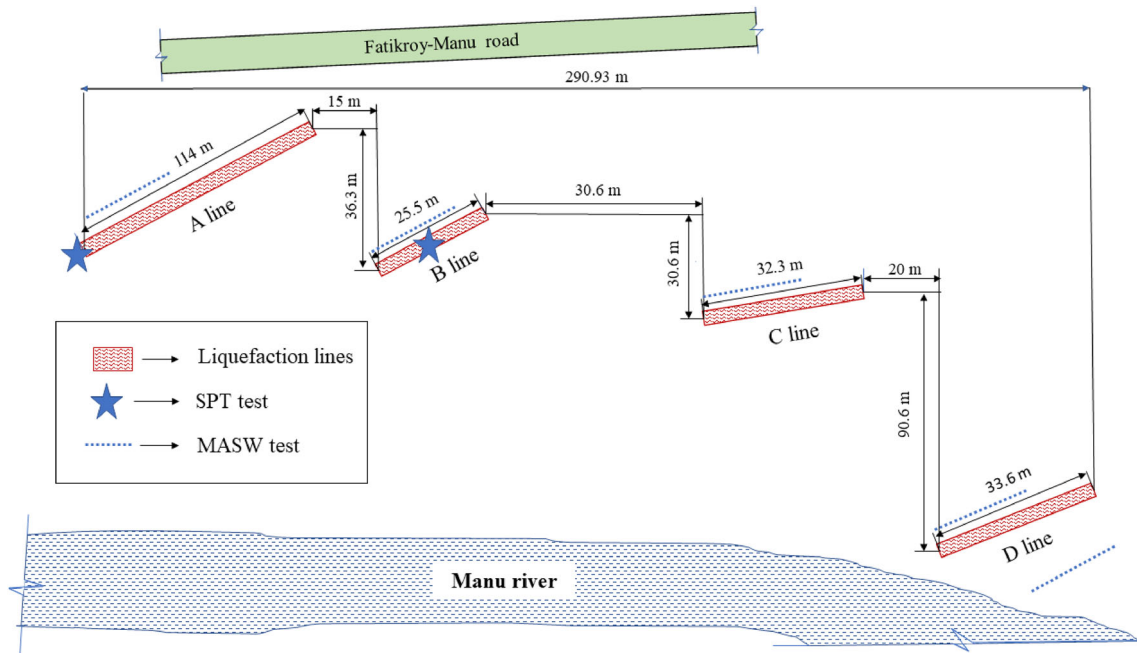


Figure 2. A schematic diagram of the liquefaction site of Tripura, India.

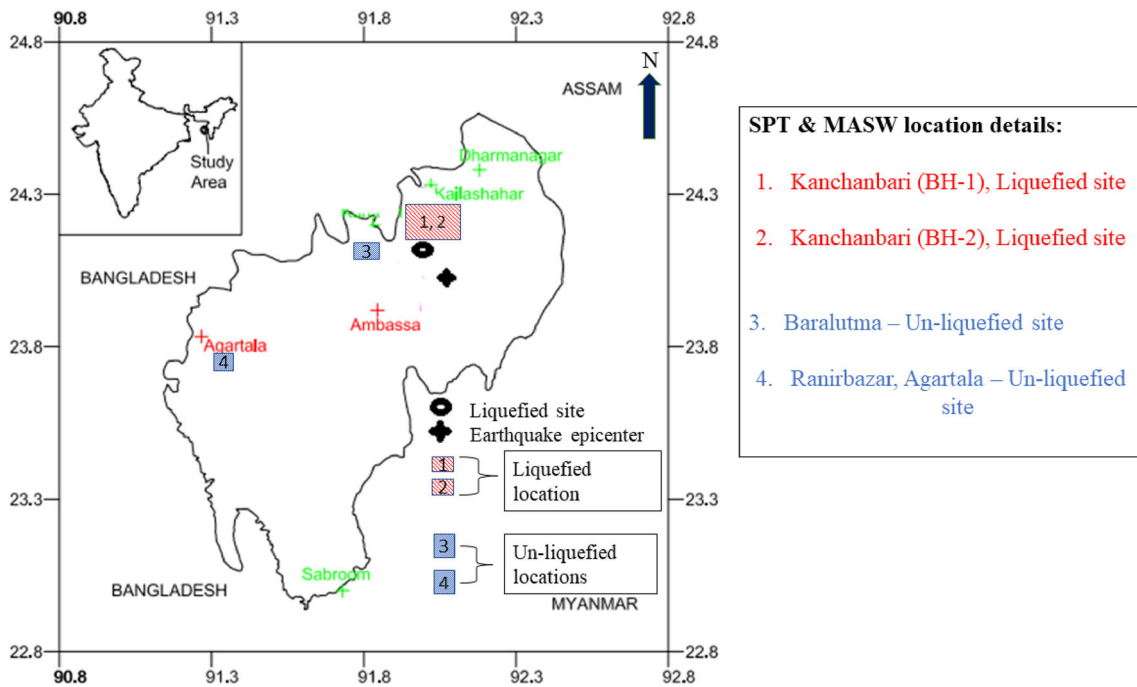


Figure 3. Study area, location of liquefaction (24.118 N, 91.991 E), epicenter of the 3rd January 2017 Tripura earthquake and SPT, MASW test locations.

3.3 Standard penetration (SPT) test

The SPT method, commonly used in field tests, was employed to check the penetration resistance of the soil and determine the liquefaction potential of the site [7]. Two SPT tests were conducted at the liquefaction site, and two

SPT data were obtained from non-liquefied areas. The SPT test setup used a 63.75 kg donut type hammer, and the lifting and dropping of the hammer were controlled manually. The hammer was released from a dropping height of approximately 75 cm. A standard split-barrel sampler was

driven about 45 cm into the soil, and the number of blows required to penetrate the last 30 cm was counted as the standard penetration resistance (N) of the soil, with the first 15 cm penetration discarded to avoid seating errors. The SPT was carried out as per Indian standard IS2131 [19], which aligns with ASTM D-1586 [20]. Figure 4 depicts one of the SPT setups in the liquefied location of A line.

The SPT was conducted at the liquefied site precisely 10 days after the occurrence of the earthquake. Borehole 1 was drilled at the starting point of line A, and borehole 2 was drilled on line B (As marked by the star symbols in figure 2), 100 m apart. Borehole 1 was bored to a depth of 30.60 m, with no rock layer found at this depth despite an SPT count of over 150. Borehole 2 was drilled up to a depth of 16 m, and the test was discontinued as the SPT N value was greater than 50. At depths of 2 meters and 1.50 meters from the ground surface, the water table was encountered in boreholes 1 and 2, respectively. Soil samples were collected at 1.5 m intervals from these boreholes, and laboratory index property tests were carried out, as detailed in section 3.5.

3.4 Liquefaction evaluation methods

In the present study, the liquefaction potential was evaluated using two field techniques: (i) a shear wave velocity-based (V_s) method employing MASW tests, and (ii) a penetration-based approach utilizing SPT N blow counts. The V_s -based method of analysis by Andrus and Stokoe [13] and Kayen *et al* [14] were adopted, and the results were compared. For the SPT-based method, the simplified procedure proposed by Idriss and Boulanger [21] was used for the liquefaction potential analysis of the sites, with relevant corrections applied, including overburden



Figure 4. Standard Penetration Test (SPT) at the liquefied location at the starting point of A-line.

correction, magnitude scaling factor, correction for SPT N measurement, and determination of cyclic stress ratio (CSR) and cyclic resistance ratio (CRR) followed by Factor of Safety (FS) calculation.

3.4.1 Shear wave velocity (V_s)-based liquefaction evaluation procedure: Andrus and Stokoe [13] proposed a method for determining the liquefaction evaluation of soil based on case history data from 26 earthquakes and shear wave velocity measurements from over 70 sites. The evaluation procedure follows a format similar to Seed and Idriss's "simplified procedure," involving the calculation of two parameters: cyclic stress ratio (CSR) and cyclic resistance ratio (CRR). CSR represents the seismic demand of the soil induced by an earthquake, while CRR represents the soil's capacity to resist liquefaction. Both parameters are used to compute the factor of safety against liquefaction (FS).

3.4.1a Estimation of CSR: To estimate CSR, the equation by Seed and Idriss [5] as expressed below is used:

$$CSR_{M,\sigma_v'} = \frac{\tau_{cyc}}{\sigma_v'} = 0.65 \frac{\tau_{max}}{\sigma_v'} = 0.65 \frac{a_{max}}{g} \frac{\sigma_v}{\sigma_v'} r_d \quad (1)$$

where, τ_{cyc} = average equivalent uniform cyclic shear stress generated by the earthquake and is expressed as 65% of the maximum induced stress, τ_{max} = maximum earthquake-induced shear stress, σ_v' = effective vertical stress at depth z , σ_v = total vertical stress at depth z , a_{max} = peak ground acceleration on the ground surface, g = acceleration due to gravity, r_d = shear stress reduction factor for adjusting the flexibility of the soil profile.

Andrus and Stokoe [13, 22] recommended using the r_d correlation same as that of the revised r_d correlation proposed by Idriss [23]:

$$r_d = \exp[\alpha(z) + \beta(z) \cdot M]$$

$$\alpha(z) = -1.012 - 1.126 \sin\left(\frac{z}{11.73} + 5.133\right) \quad (2)$$

$$\beta(z) = 0.106 + 0.118 \sin\left(\frac{z}{11.28} + 5.142\right)$$

here z represents the depth below the ground surface in meters, and the arguments inside the sin terms are in radian.

3.4.1.b Estimation of CRR: Andrus and Stokoe [13, 21] proposed the following equation for calculating the cyclic resistance ratio of the soil:

$$CRR = \left\{ a \left(\frac{V_{s1}}{100} \right)^2 + b \left(\frac{1}{V_{s1}^* - V_{s1}} - \frac{1}{V_{s1}^*} \right) \right\} MSF \quad (3)$$

where V_{s1} is the corrected value of shear wave velocity for overburden pressure to a reference of 1 atm, V_{s1}^* is the limiting upper value of V_{s1} for cyclic liquefaction occurrence, a and b are curve fitting parameters, and MSF is the magnitude scaling factor.

The overburden corrected shear wave velocity, V_{s1}

$$V_{s1} = V_s * \left(\frac{P_a}{\sigma_v'} \right)^{0.25} \quad (4)$$

where, P_a = Atmospheric pressure (equals to approximately 100 kPa), σ_v' = Initial effective vertical stress.

The limiting value V_{s1}^* is depends on the FC and the relationship for V_{s1}^* based on FC is as follows:

$$V_{s1}^* = 215 \text{ m/s, for sands with } FC \leq 5\% \quad (5a)$$

$$V_{s1}^* = 215 - 0.5 * (FC - 5) \text{ m/s, for sands with } 5\% < FC < 35\% \quad (5b)$$

$$V_{s1}^* = 200 \text{ m/s, for sands and silts with } FC \geq 35\% \quad (5c)$$

here, FC represents the average fine content in percentage by mass.

The magnitude scaling factor (MSF), as revised by Idriss [23], is expressed as:

$$MSF = 6.9 \exp \frac{-M_w}{4} - 0.06, \text{ for } M_w > 5.2 \quad (6a)$$

$$MSF = 1.82, \text{ for } M_w \leq 5.2 \quad (6b)$$

3.4.1c Estimation of CSR and CRR (by Kayen et al [14]): Earlier studies on liquefaction analysis based on shear wave velocity (V_s) lacked velocity profiles in deeper soil deposits (>10 m). To address this limitation, Kayen et al [14] compiled a comprehensive global (V_s) dataset by collecting new data from liquefaction-evaluation sites in Japan, Taiwan, China, India, and the United States (US), comprising 300 sites. They subsequently proposed an alternative approach to soil liquefaction analysis.

For evaluating the cyclic stress ratio (CSR), Kayen et al [14] recommended employing the depth reducing factors (r_d) introduced by Cetin et al [24]. Additionally, Kayen et al [14] introduced a new correlation for the magnitude scaling factor (MSF), referred to as the earthquake duration weighting factor (DWF), expressed as follows:

$$DWF = 15 * M^{-1.342} \quad (7)$$

This duration weighting factor (DWF or MSF) was developed using various approaches, utilizing cyclic laboratory testing and/or field case history data from different investigators. The model is valid for magnitudes $5.5 < M_w < 9.0$.

Moreover, Kayen et al [14] proposed a CRR correlation based on the Probability of Liquefaction (P_L) as follows:

$$P_L = \emptyset - \left\{ \frac{(.0073.V_{s1})^{2.8011} - 1.946.\ln(CSR)}{.4809} - \frac{-2.6168.\ln(M_w) - .0099.\ln(\sigma_v') + .0028.FC}{.4809} \right\} \quad (8)$$

$$CRR = \exp \left\{ \frac{(.0073.V_{s1})^{2.8011} - 2.6168.\ln(M_w)}{1.946} - \frac{.0099.\ln(\sigma_v') + .0028.FC - .4809.\emptyset^{-1}(P_L)}{1.946} \right\} \quad (9)$$

For the deterministic approach, the P_L value proposed by Kayen et al [14] should be considered as 15 %.

3.4.2 Factor of safety against liquefaction: The factor of safety against liquefaction is defined as a ratio between CRR and CSR, and can be expressed as:

$$FS = \frac{CRR}{CSR_{M=7.5, \sigma_{vm}=1atm}} \quad (10)$$

As a general guideline, an FS value less than 1 predicts the soil to be liquefiable, while an FS value greater than 1 predicts the soil to be non-liquefiable. Acceptable factors of safety can vary between approximately 1.2 and 1.5, although FS values outside this range may sometimes be acceptable based on the project's importance [6].

3.4.3 Assessment of liquefaction potential index (LPI): The liquefaction potential index (LPI) is a useful way to describe liquefaction potential. It is an index used to quantify the degrees of severity of the entire soil column and predicts whether manifestation of liquefaction feature will occur at the ground surface or not. Although, factor of safety (FS) is a useful parameter to predict whether a soil layer is prone to liquefaction or not, however, it does not quantify the damage expected from liquefaction or its severity. Hence, LPI was originally developed by Iwasaki et al [25] to predict the potential of liquefaction to cause foundation damage at sites in Japan. Later, LPI was modified by Luna and Frost [26], MERM [27], Sonmez et al [28] as given in table 1. LPI proposed by Sonmez and Goceoglu [28] is expressed as follows:

$$LPI = \int_0^{20} F(z).w(z)dz \quad (11)$$

where,

$$F(z) = 1 - FS, \text{ for } FS \leq .95$$

$$F(z) = 0, \text{ for } FS \geq 1.2$$

$$F(z) = 2 \times 10^6 e^{-18.427FL} \text{ for } .95 < FS < 1.2$$

And $w(z)$ is the depth weighting factor which is given as:

$$w(z) = 10.5z,$$

Where z is the depth at the midpoint of the soil layer in meters.

Table 1. Liquefaction potential classification modified by Luna and Frost, MERM, and Sonmez [26–28].

| LPI | Iwasaki <i>et al</i> (1982) | Luna and Frost (1998) | MERM (2003) | Sonmez (2005) |
|-------------------|-----------------------------|-----------------------|-------------|---|
| LPI = 0 | Very low | Little to none | None | Non-liquefiable (Based on $FS \geq 1.2$) |
| $0 < LPI \leq 2$ | – | – | – | Low |
| $2 < LPI \leq 5$ | – | – | – | Moderate |
| $0 < LPI \leq 5$ | Low | Minor | Low | – |
| $5 < LPI \leq 15$ | High | Moderate | Medium | High |
| $LPI > 15$ | Very high | Major | High | Very high |

3.5 Laboratory investigations of the liquefied site soil properties

The ejected soil samples obtained from the liquefied site (Kanchanbari) of Tripura were sieved carefully and laboratory index property tests were carried out. Figure 5 shows the Grain Size Distribution (GSD) of the surface deposited liquefied soil and the corresponding index properties are enumerated in table 2. It contained 79.75 % of fine sand, 19.83 % of silt, and 0.41 % of clay content with a specific gravity of 2.64. The soil is non-plastic in nature and classified as silty sand (poorly graded) according to IS: 2720 [29] and Unified Soil Classification System [30]. Additionally, the GSD curve of the erupted soil deposit was compared with widely accepted grain size distribution curves for potentially liquefiable soil as proposed by Tsuchida [31], confirming that the present liquefied soil deposits fell within the ranges of the most liquefiable boundaries. A Scanning Electron Microscope (SEM) image of the liquefied soil is shown in figure 6, revealing that the particles exhibited sub-angular to sub-rounded characteristics.

The in-situ soil properties of the liquefied site obtained through the SPT boreholes and laboratory test are

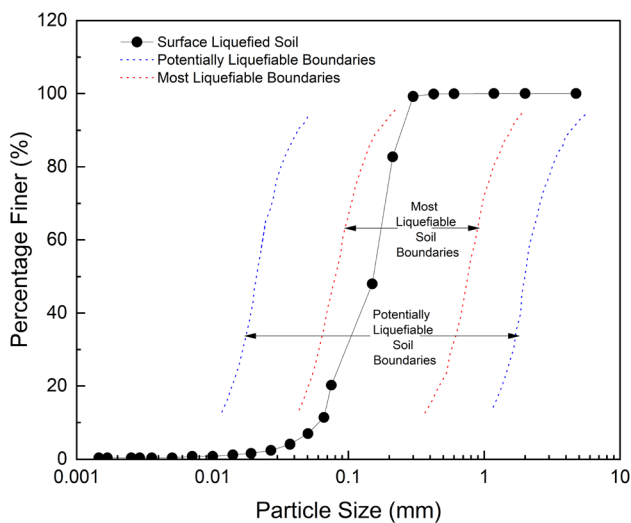


Figure 5. Grain size distribution of the ejected soil deposits of the 2017 Tripura earthquake, India.

Table 2. Index properties of the liquefied surface soil obtained from Kanchanbari, Tripura, India.

| Sl. no. | Soil properties | Unit | Value |
|---------|-----------------------------------|------|-------------|
| 1 | Specific gravity | – | 2.64 |
| 2 | Particle size distribution | | |
| | (a) Gravel | % | 0 |
| | (b) Sand | % | 79.75 |
| | (c) Fines (silt & clay) | % | 20.25 |
| | (d) Silt | % | 19.84 |
| | (e) Clay | % | 0.41 |
| | (f) Cu (uniformity coefficient) | – | 2.90 |
| | (g) Cc (coefficient of curvature) | – | 0.86 |
| 3 | Liquid limit | % | 28.89 |
| 4 | Plastic limit | – | Non-plastic |
| 5 | Maximum void ratio | – | 0.886 |
| | Minimum void ratio | – | 0.517 |
| 6 | Soil classification (USCS) | – | Silty-sand |

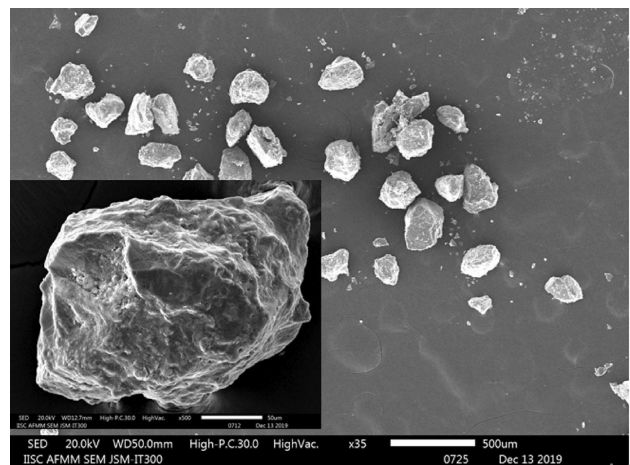


Figure 6. Scanning Electron Microscope (SEM) image of the surface liquefied soil of Tripura.

summarized in tables 3 and 4. An undisturbed sample was also collected using a thin Shelby tube sampler from a depth of 3 m and in-situ dry density was measured as 1.66 g/cc. The estimated maximum and minimum relative density were 1.74 g/cc and 1.40 g/cc, respectively. The

Table 3. In-situ soil property and soil profile of the liquefied site obtained from SPT bore hole 1.

| Depth (m) | Soil color | Soil description | Index Properties | | | | | | | | | | Soil classification |
|-------------|------------------------|-------------------------------------|------------------|----------|-----------|----------|----------|--------|--------|------|---|---|---------------------|
| | | | G | Sand (%) | Fines (%) | Silt (%) | Clay (%) | LL (%) | PL (%) | P | | | |
| 1.00–1.50 | Brownish | Clay soil with silt | 2.65 | 9.55 | 90.45 | 80.33 | 10.12 | 26.34 | 19.78 | 6.57 | | | CL-ML |
| 3.0–4.50 | Light whitish/brownish | Sandy soil with some stress of silt | 2.64 | 95.50 | 4.50 | – | – | – | – | – | – | – | SP |
| 4.5–5.0 | | | 2.66 | 92.00 | 8.00 | – | – | 22.03 | NP | – | – | – | SP-SC |
| 6.00–7.50 | | | 2.64 | 77.00 | 23.00 | – | – | 20.36 | NP | – | – | – | SC |
| 7.50–9.00 | | | 2.61 | 75.5 | 24.5 | – | – | 21.5 | NP | – | – | – | SC |
| 9.00–10.50 | | | 2.66 | 90.5 | 9.5 | – | – | 25.23 | NP | – | – | – | SP-SC |
| 10.50–12.00 | | | 2.66 | 83 | 17 | – | – | 18.06 | NP | – | – | – | SC |
| 12.00–13.50 | | | 2.68 | 93.5 | 6.5 | – | – | 21.80 | NP | – | – | – | SP-SC |
| 13.50–15.00 | | | 2.65 | 6.5 | 93.5 | 45.78 | 47.72 | 19.99 | 16.55 | 3.44 | – | – | CL-ML |
| 15.00–16.50 | | | 2.65 | 20 | 80 | 66.5 | 13.5 | 27.76 | 19.98 | 7.78 | – | – | CL-ML |
| 16.50–18.00 | Grey | Clay soil with silt | 2.65 | 95 | 5 | – | – | 25.9 | NP | – | – | – | SP-SC |
| 18.00–19.50 | Whitish | Sandy soil | 2.64 | 65.5 | 34 | – | – | 26.9 | 20.2 | 6.7 | – | – | CL-ML |
| 19.50–21.00 | | | 2.65 | 95.5 | 4.5 | – | – | 28.21 | NP | – | – | – | SP |
| 21.00–22.50 | | | 2.65 | 94.5 | 5.5 | – | – | 25.7 | NP | – | – | – | SP-SC |
| 22.50–24.00 | | | 2.65 | 91.5 | 8.5 | – | – | 24.9 | NP | – | – | – | SP-SC |
| 24.00–25.50 | | | 2.65 | 91 | 9 | – | – | 22.1 | NP | – | – | – | SP-SC |
| 25.50–27.00 | | | 2.65 | 89 | 11 | – | – | 26.4 | NP | – | – | – | SP-SC |
| 27.00–28.50 | | | 2.66 | 92.5 | 7.5 | – | – | 25.5 | NP | – | – | – | SP-SC |
| 28.50–30.00 | | | 2.67 | 90.5 | 9.5 | – | – | 25.20 | NP | – | – | – | SP-SC |
| 30.00–30.60 | | | 2.64 | 84 | 16 | – | – | 22.2 | NP | – | – | – | SC |

Table 4. In-situ soil property and soil profile of the liquefied site obtained from SPT bore hole 2.

| Depth (m) | Soil color | Soil description | Index properties | | | | | | | PI | Soil classification |
|-----------|------------------------|---------------------|------------------|----------|-----------|----------|----------|--------|--------|------|---------------------|
| | | | G | Sand (%) | Fines (%) | Silt (%) | Clay (%) | LL (%) | PL (%) | | |
| 0.5–2.0 | Light brownish | Clay soil with silt | 2.65 | 8.00 | 92.00 | 82.59 | 9.41 | 24.52 | 18.24 | 6.28 | CL-ML |
| 2.0–3.5 | | | 2.64 | 95.50 | 4.50 | – | – | – | NP | – | SP |
| 3.5–5.0 | | | 2.64 | 95.50 | 4.50 | – | – | – | NP | – | SP |
| 5.0–6.5 | Light whitish/brownish | Sandy clay soil | 2.66 | 93.00 | 7.00 | – | – | 21.2 | NP | – | SP-SC |
| 6.5–7.0 | | | 2.61 | 77.50 | 22.50 | – | – | 20.60 | NP | – | SC |
| 7.0–8.5 | | | 2.68 | 88.5 | 11.5 | – | – | 26.20 | NP | – | SP-SC |
| 8.5–10.0 | Light brownish | Sandy soil | 2.66 | 91.5 | 8.5 | – | – | 23.34 | NP | – | SP-SC |
| 10.0–11.5 | | | 2.65 | 82.5 | 17.5 | – | – | 18.04 | NP | – | SC |
| 11.5–13.0 | | | 2.65 | 93.00 | 7.00 | – | – | 21.20 | 16.55 | 4.65 | SP-SC |
| 13.0–14.5 | Light whitish | Clay soil with silt | 2.64 | 8.50 | 91.50 | 47.17 | 44.33 | 18.66 | 15.45 | 3.21 | CL-ML |
| 14.5–16.0 | | | 2.64 | 15.00 | 75.00 | 61.48 | 13.52 | 26.21 | 17.72 | 8.49 | CL-ML |
| 16.0–17.5 | | | 2.66 | 92.50 | 7.50 | – | – | 25.00 | NP | – | SP-SC |

borehole data (as presented in tables 3 and 4), revealed the presence of a variety of soils at different depths, including clean sands (SP), clayey sands (SC), silty clays (CL-ML), and poorly graded sand with clay (SP-SC). The site was characterized by a shallow water table depth and the presence of poorly graded sand and clayey sand between depths of 3 and 8 meters, rendering it more susceptible to liquefaction.

4. Results and discussion

The initial section of the results focuses on the analysis of two field methods, MASW and SPT tests, which were conducted at both the liquefaction site and non-liquefied sites to assess the soil profile strength and the presence of liquefiable layers following the 2017 Tripura earthquake, India. The factor of safety against liquefaction using SPT-based methods - Andrus and Stokoe [13, 21] and Kayen *et al* [14] is compared and discussed. In the later part of the results, an evaluation of the liquefaction potential index (LPI) for the surface liquefied site is undertaken to investigate the likelihood of liquefaction features manifesting at the ground surface.

4.1 Investigation of the liquefied site using shear wave velocity measurement by MASW

Figure 7a and b show the typical dispersion curve estimation and inversion analysis curve obtained from one of the MASW tests at the liquefaction site. A total of five MASW tests were carried out at the liquefied location (on A, B, C, D, E lines as presented in figure 2) where linear sand boils were observed. The results of the processed V_s profiles with respect to depths are presented in figure 8a. Additionally, to

better understand the properties of the ground at the liquefied location, MASW tests were conducted at two non-liquefied sites (as depicted by the blue rectangular symbols in figure 3), and the results of these tests are shown in figure 8b.

The shear wave velocity profiles (Figure 8a) indicate that at the liquefaction site, the V_s values are observed to be less than 220 m/s up to a depth of 12 m to 15 m for all five tests. Beyond this depth, a significant variation in the shear wave velocity measurement is noticed. Up to 7.5 m, the V_s values are less than 150 m/s, suggesting that the site is characterized by soft soil conditions and is susceptible to liquefaction. The majority of the shear wave velocity values at the liquefaction site fall within the range of 53 to 360 m/s. Furthermore, the V_s 30 value determined using the National Earthquake Hazards Reduction Program (NEHRP) [32] site classification for the liquefied site of Tripura reveals that the site falls under Site Class D ($180 \text{ m/s} \leq V_s \leq 360 \text{ m/s}$). In contrast, the shear wave velocity values are greater at the non-liquefied sites (as shown in figure 8b) compared to the liquefied site.

4.2 Investigation of the liquefied site using SPT measurement

Figure 9a depicts the variation of SPT N values with depth for boreholes 1 and 2 at the liquefaction site. The data reveals that the observed SPT N values in the boreholes are very low in the topsoil layer, i.e., below a depth of 8 m, despite the site having experienced liquefaction during the 2017 Tripura earthquake. The SPT N values range from 1 to 7 up to a depth of about 15 m (in the case of borehole 2), after which it abruptly increases to more than 50. This suggests that the entire soil column unit (up to 15 m)

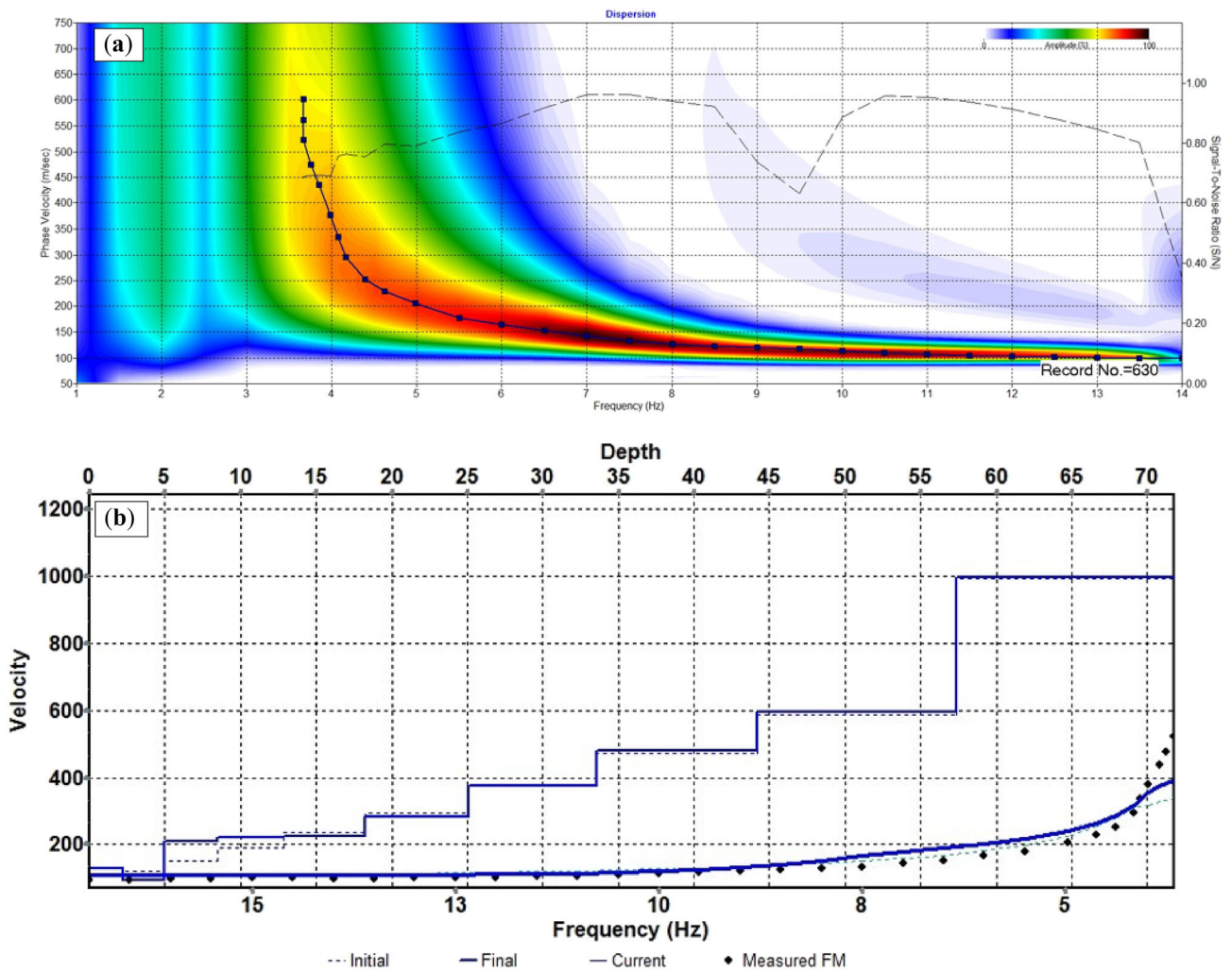


Figure 7. (a) Typical dispersion curve estimation and (b) inversion analysis curve from MASW test.

appears to have a high potential for liquefaction during earthquakes.

Interestingly, it is commonly believed that once a site is liquefied, the soil particles rearrange, resulting in densification that makes the soil less susceptible to re-liquefaction in subsequent events. However, the SPT site investigation at the liquefied site reveals low penetration resistance at shallow depths, indicating that the site still possesses a high chance of re-liquefaction during future earthquakes.

Figure 9b displays the variation of SPT N with depth for the other two non-liquefied sites. The penetration resistance N , at the non-liquefied sites exhibits slightly higher values compared to the liquefied site. However, its value remains less than 20 within the top 8 meters of depth at the non-liquefied sites. As shown in figure 8b, a sharp increase in shear wave velocity measurements can also be seen at shallow depths for these non-liquefied locations. This agreement between SPT N and MASW measurements

suggests that combining SPT and MASW tests can yield promising results.

The low SPT N values observed after liquefaction can be attributed to several factors. Firstly, historical flood deposits from the Manu River, which flowed through the area five to six decades ago, have formed a very loose deposition beneath the surface of the site. This area, now used for agriculture, consists of loose soils with minimal over-consolidation or overburden pressure, and a high fines content, such as silt and clay (refer tables 3 and 4). These fine-grained soils inherently exhibit lower SPT N values, especially after liquefaction. It can also be noted that the earthquake that triggered the liquefaction was of moderate magnitude (M_w 5.7), which may not have caused significant densification or particle rearrangement at the site.

Secondly, residual excess pore pressures and non-uniform densification across the site can greatly influence SPT N values. Although some pore pressure dissipation occurs, it may not be complete, leaving residual pressures that

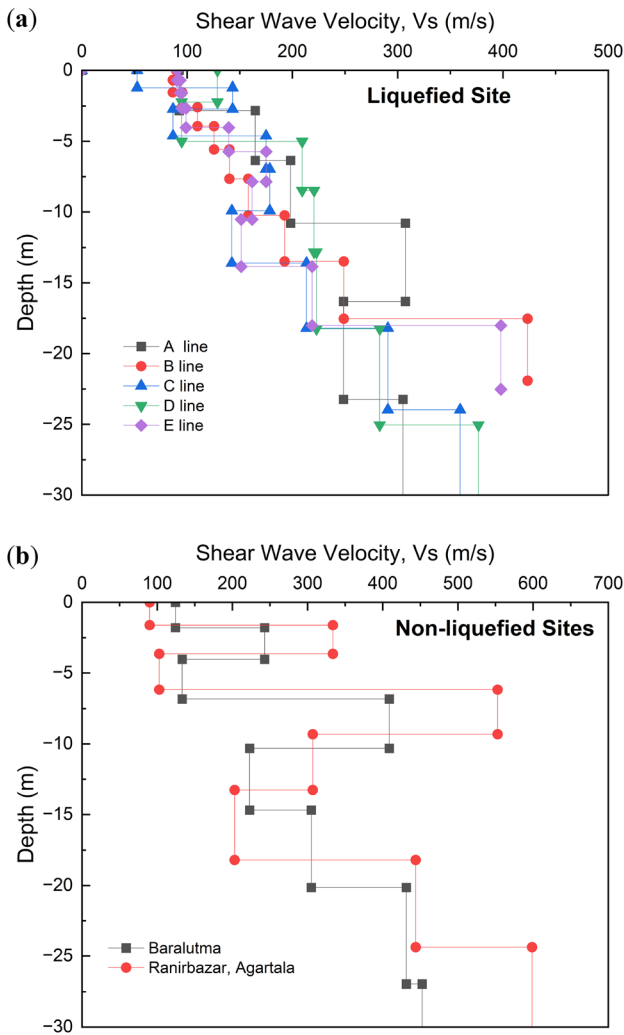


Figure 8. (a) Shear wave velocity profile with respect to depth at the liquefied site and (b) non-liquefied locations retrieved from MASW test.

inhibit effective stress buildup within the soil. This residual pore pressure can reduce soil strength and resistance, resulting in lower SPT N values even after the initial liquefaction event. Liquefaction also alters soil structure, causing particle rearrangement that can initially result in a loose structure with poorly established contact points, further contributing to lower penetration resistance in SPT tests.

These factors collectively suggest that the site remains susceptible to re-liquefaction, as the soil has not gained significant strength post-event. This is consistent with studies such as Seed (1986), which shows that sites with low post-liquefaction SPT N values have a higher propensity for re-liquefaction [33].

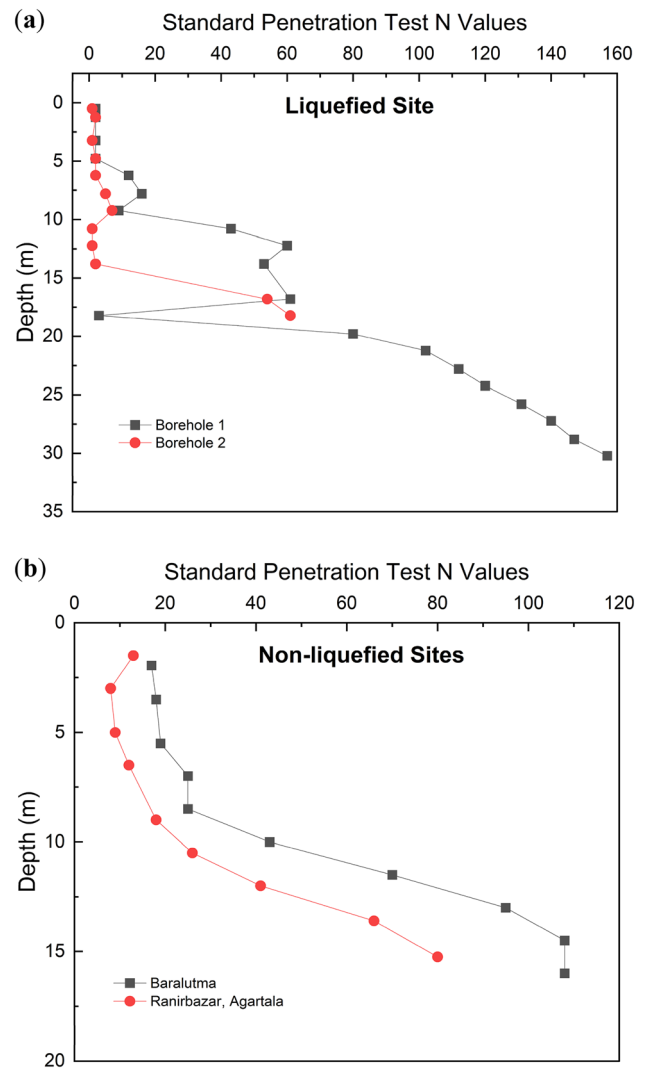


Figure 9. (a) The SPT N variation with respect to depth obtained for liquefied site (borehole 1 and 2) and (b) un-liquefied sites.

4.3 Suspected liquefiable layer during 3rd January 2017 Tripura earthquake

The SPT penetration resistance values presented in figure 9a fall as low as 1 blow for borehole 1 and less than 10 blows for borehole 2 at depths lower than 8 m. This indicates that the resistance to liquefaction in these soil layers is extremely low, corresponding to a sand relative density well below 50% [34]. Additionally, the shallow water table depth of 1.5 to 2 meters at the liquefaction site during the 2017 Tripura earthquake significantly increased the site’s susceptibility to liquefaction. A shallow water table makes soil more prone to liquefaction because water can easily rise to the surface during an earthquake, reducing soil strength. In contrast, a deeper water table reduces the likelihood of liquefaction by making it more difficult for water to reach the surface.

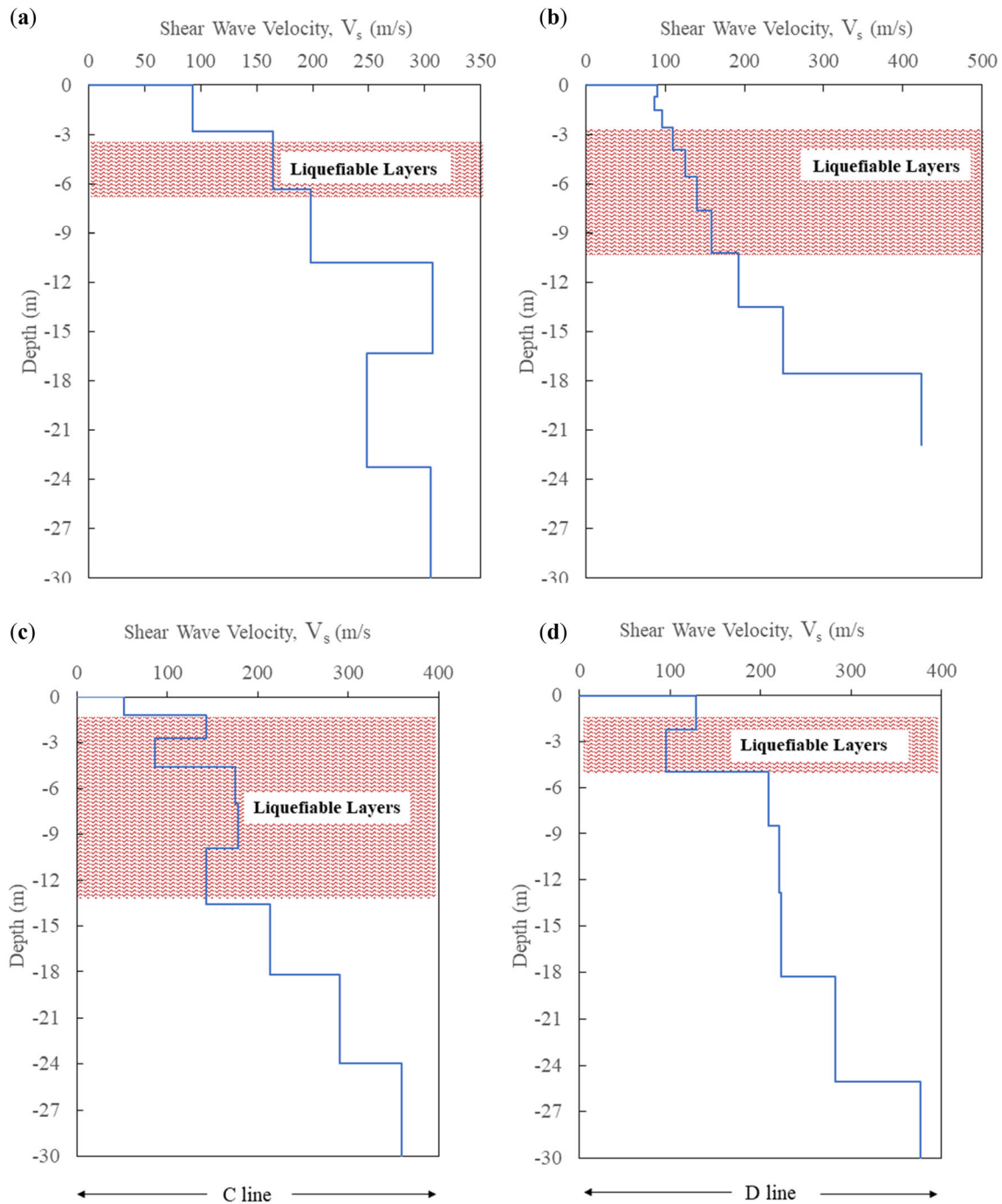


Figure 10. Variability of the V_s profile at the liquefied location along the linear sand boil lines-A, B, C, and D.

Liquefaction occurs when cyclic shear stresses from an earthquake cause the soil particles to rearrange, leading to a buildup of excess pore water pressure. When this pressure equals the overburden pressure, the soil loses its strength and stiffness, resulting in liquefaction. During the 2017 Tripura earthquake, the shallow water table provided a ready source of water, facilitating the buildup of excess pore water pressure during the shaking.

Corresponding to the subsoil profile at the investigation site, as shown in tables 3 and 4, the first 1.00 to 1.50 m is classified as CL-ML, with 80% silt, 10% clay, and 10% sands. The next 3 to 5 m is classified as SP, followed by SC, SP-SC (between the depth of 6.00 m to 13.00 m), and CL-ML at a depth of 13.50 m to 16.50 m. This indicates that the poorly graded sand at a depth of 3 to 13 m is sandwiched between the silty clay layer deposits, and a mixture of sand

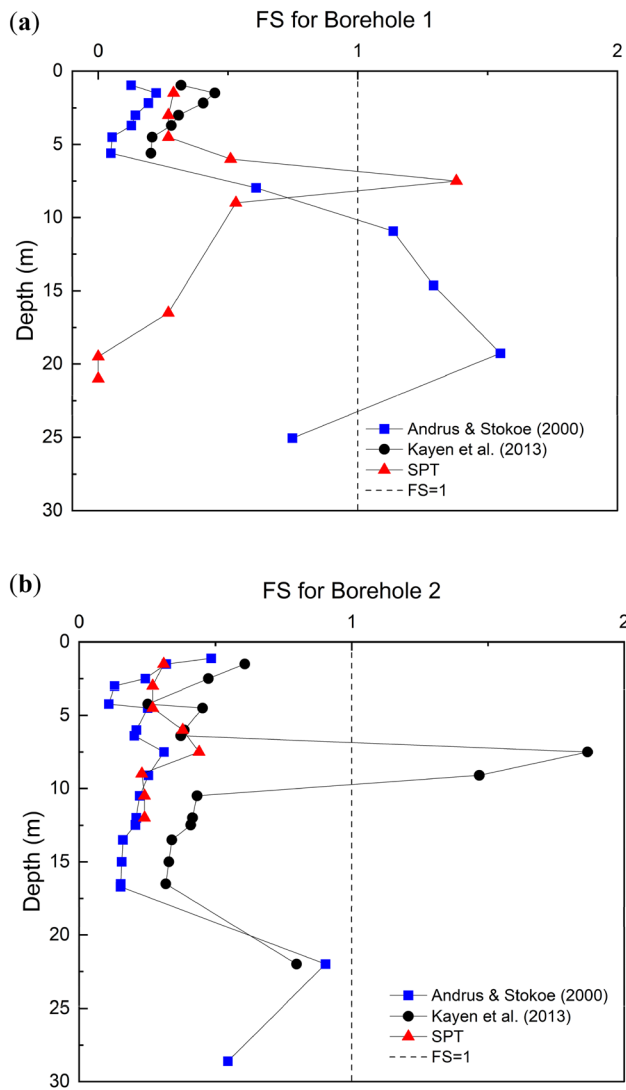


Figure 11. Variation of re-liquefaction factor of safety (FS) with depth obtained using V_s and SPT data at the liquefied site.

grain and water is rushed towards the ground surface during the earthquake, transporting fine particles of the upper layer soils. This phenomenon could explain why fine sands (80%) with an appreciable percentage of fines (about 20%) were ejected and deposited on the surface due to liquefaction during the 2017 Tripura earthquake.

Furthermore, the variability of the V_s profile resulting from the MASW tests obtained for A, B, C, and D lines at the liquefaction site are presented separately in figure 10. It

should be noted that V_s values are less than 150 m/s at depths below 6 m for A-line, below 8 m for B-line, below 6 m for C-line, and below 5 m for D-line, respectively. According to Stokoe *et al* [11], sandy soil with $V_s \leq 180$ m/s is prone to liquefaction during earthquakes. Another study by Andrus *et al* [21] also suggests that sandy layers with a corrected V_s value less than 215 m/s are highly susceptible to liquefaction. Therefore, the shear wave velocity values less than or equal to 180 m/s below a depth of 8 m suggest that the stiffness of the site at these depths is soft and vulnerable to liquefaction. The observed SPT penetration resistance is also very low within these soil layers, indicating that the potential liquefiable layer lies between 3 and 8 m. Hence, field investigations and laboratory tests support that liquefaction occurred in loose fine sands and silts deposited in the channel floodplain area.

4.4 Re-liquefaction analysis of liquefied site

In order to investigate the re-liquefaction possibility of liquefied site of Tripura, in-situ experimental data obtained from MASW and SPT were utilized. The Cyclic Stress Ratio (CSR) and Cyclic Resistance Ratio (CRR) for the liquefied site were calculated using equations (1) through (9). For the V_s -based analysis, the method proposed by Andrus and Stokoe [13] and Kayen *et al* [14] was adopted. For the SPT N-based analysis, the methodology by Idriss and Boulanger [22] was employed, and necessary correction factors for SPT N measurement were applied (such as energy correction factor = 0.60 for donut type, borehole diameter correction = 1.05, liner correction = 1). The factor of safety against liquefaction for a chosen magnitude and acceleration was then determined using equation (10).

Anbazhagan *et al* [15] highlighted the possible variation of surface peak ground acceleration (PGA) at the liquefaction site based on the intensity values reported from the earthquake. A maximum surface PGA of 0.28 g was assessed at the liquefied site, while the expected PGA according to IS1893 was 0.36 g [18]. Considering that the site had already experienced liquefaction for a PGA of 0.28 g, a surface PGA of 0.36 g was considered for the re-liquefaction analysis in the present study. The CSR for the sites was estimated using a PGA of 0.36 g for a chosen earthquake magnitude of $M = 7.5$.

Figure 11a and b show the plot of the re-liquefaction factor of safety (FS) with respect to depth for the liquefied site. It is interesting to note (from figure 11a and b) that the

Table 5. Site classification and liquefaction potential analysis of the liquefied site of Tripura.

| Site name | V_s^{30} (m/s) | Site class | LPI (Sonmez 2003) |
|---|------------------|------------|-------------------------|
| 1. Kanchanbhari (BH-1) (Liquefied site) | 194 | D | Very high (LPI = 34.4) |
| 2. Kanchanbhari (BH-2) (Liquefied site) | 185 | D | Very high (LPI = 46.37) |

FS against liquefaction resulting from the V_s -based method - Kayen *et al* [14] matches well with that of the SPT-based analysis. However, the factor of safety resulting from Andrus *et al* [21] predicts a much lower value of FS than those of Kayen *et al* [14] and the SPT-based method, providing the most conservative results. At the liquefied site (figure 11a and b), FS values less than 1 at a shallower depth ($\sigma'_v < 100$ kPa) for both SPT and V_s -based methods indicate that soil layers at these depths are prone to liquefaction.

The corresponding Liquefaction Potential Index (LPI) for the liquefied site is calculated by integrating FS with depth using Eq. (11) given by Sonmez [28]. Liquefaction is most likely to occur for sites with $LPI > 15$, and liquefaction susceptibility is very unlikely for sites with $LPI < 2$. The estimated LPI along with site classes are summarized in table 5. According to the NEHRP [32], the liquefied site falls under the category of 'site class D' ($180 \text{ m/s} \leq V_s \leq 360 \text{ m/s}$). The LPI values show very high values (i.e., LPI is greater than 15) at the liquefaction site for both boreholes 1 and 2. These results once again confirm the evidence of liquefaction occurrence during the 2017 Tripura earthquake. Furthermore, the V_s 30 value remains very low even though the site had previously experienced liquefaction, indicating the possibility of re-liquefaction. Thus, the estimated LPI study reveals that a high degree of liquefaction damage could be expected at the site during future earthquakes of greater magnitudes.

It is important to note that one of the primary challenges encountered during this study was the limited historical data on past earthquake-induced liquefaction events in Tripura and the absence of a region-specific Cyclic Resistance Curve or liquefaction strength curve. The authors recommend further investigations to compile a comprehensive database of past liquefaction occurrences and to develop a cyclic strength curve for Tripura. Additionally, detailed geotechnical and geophysical investigations in Agartala and areas near the Dauki and Madhupur faults (North Tripura zone), including micro-zonation studies, are recommended. These regions share similar soil characteristics and proximity to active fault zones, potentially making them susceptible to liquefaction events. These efforts would significantly contribute to creating more robust liquefaction hazard assessment and mitigation strategies tailored to the area.

5. Summary and conclusions

The 2017 Tripura earthquake, with a moment magnitude of M_w 5.7, provided the first documented evidence that a moderate-magnitude earthquake can induce liquefaction in the region, a phenomenon usually associated with stronger earthquakes. This study is significant due to the scarcity of case histories documenting in-situ soil properties at

liquefaction sites triggered by earthquakes below magnitude 6. The key findings of this study are outlined below.

- Conventional wisdom suggests that once a site undergoes liquefaction, soil particles rearrange, leading to densification that reduces susceptibility to re-liquefaction in subsequent events. However, field investigations using MASW and SPT techniques revealed unexpected findings at the liquefied site. Low shear wave velocity ($V_s \leq 180$ m/s) and penetration resistance at shallow depths (2 to 7 counts below a depth of 8 m) were observed, indicating that the site retains a high susceptibility to re-liquefaction during future earthquakes.
- The soil basic index test revealed that the soil profile at the liquefied site comprised silty clay in the upper (1.00 to 1.5 m) and lower layers (13 to 16 m), with poorly graded sand and clayey sand in between. This stratification suggests that during the earthquake, the thick sandy soil deposit was sandwiched between the clay layers, leading to liquefaction between depths of 3 and 8 m. The site's susceptibility to liquefaction was further exacerbated by the water table's location, which was between 1.5 and 2 meters below the ground surface.
- At the liquefied site, FS values less than 1 at a shallower depth ($\sigma'_v < 100$ kPa), from both SPT and V_s based methods indicate that soil layers at these depths are prone to liquefaction. Andrus and Stokoe [13] method provided more conservative results, while V_s -based method predicted slightly higher FS at shallower depths.
- The liquefaction potential index (LPI) values of 34.4 and 46.37 at the Kanchanbari liquefaction site indicate a 'very high' severity (site class D), with a strong potential for re-liquefaction. This critical hazard requires thorough geotechnical investigations, improved design practices, and continuous monitoring. Future seismic hazard assessments should prioritize liquefaction hazards as one of the essential components in seismic zonation and risk mapping.

These findings collectively highlight the site's high susceptibility to liquefaction, emphasizing the need to consider the residual strength of liquefied soils in design and the importance of comprehensive geotechnical investigations. A detailed geotechnical and geophysical investigations in Agartala and areas proximity to active fault zones such as Dauki and Madhupur faults (North Tripura zone), including micro-zonation studies, are recommended.

List of symbols

| | |
|-------|---------------------------------|
| M_w | Moment magnitude |
| V_s | Shear wave velocity |
| N | Standard penetration resistance |

| | |
|------------|--|
| M | Earthquake magnitude |
| V_s^{30} | Average shear wave velocity of the top 30 meters of soil or rock |
| SPT | Standard penetration test |
| MASW | Multichannel analysis of surface wave |
| LPI | Liquefaction potential index |
| SWV | Surface wave velocity |
| CPT | Cone penetration test |
| BH | Borehole |
| PGA | Peak ground acceleration |
| CSR | Cyclic stress ratio |
| CRR | Cyclic resistance ratio |
| FS | Factor of safety |

Acknowledgements

This work was supported by the “Board of Research in Nuclear Sciences (BRNS)”, Department of Atomic Energy (DAE), Government of India under Grant Sanction No 36(2)/14/16/2016-BRNS for the project titled “Probabilistic seismic hazard analysis of Vizag and Tarapur considering regional uncertainties”. Authors thank Mr. Ayush Agrawal, M. Tech scholar at IISc for assisting in carrying out MASW tests at sites.

Data availability

All the data can be made available from the corresponding author by request.

Declarations

Conflict of interest The authors declare that there is no conflict of interest.

References

- [1] Kramer S L 1996 Geotechnical earthquake engineering. vol 1. Pearson Education, India, pp 1–17
- [2] Maurya D M, Goyal B, Patidar A K, Mulchandani N, Thakkar M G and Chamyal L S 2006 Ground penetrating radar imaging of two large sand blow craters related to the 2001 Bhuj earthquake, Kachchh, Western India. *J. Appl. Geophys.* 60: 142–152
- [3] Kaiser A, Holden C, Beavan J, Beetham D, Benites R, Celentano A, Collett D, Cousins J, Cubrinovski M, Dellow G and Denys P 2012 The Mw 6.2 Christchurch earthquake of February 2011: preliminary report. *N. Z. J. Geol. Geophys.* 55: 67–90
- [4] Sharma K and Deng L 2019 Reconnaissance report on geotechnical engineering aspect of the 2015 Gorkha, Nepal, earthquake. *J. Earthq. Eng.* 23: 512–537
- [5] Seed H B and Idriss I M 1971 Simplified procedure for evaluating soil liquefaction potential. *J. Soil Mech. Found. Div.* 97: 1249–1273
- [6] Seed H B and Idriss I M 1982 Ground Motions and Soil Liquefaction during Earthquakes. *Earthquake Engineering Research Institute Monograph, Oakland*
- [7] Seed H B, Idriss I M and Arango I 1983 Evaluation of liquefaction potential using field performance data. *J. Geotech. Eng.* 109: 458–482
- [8] Youd T L and Idriss I M 2001 Liquefaction resistance of soils: summary report from the 1996 NCEER and 1998 NCEER/NSF workshops on evaluation of liquefaction resistance of soils. *J. Geotech. Geoenviron. Eng.* 127: 297–313
- [9] Robertson P K and Wride C E 1998 Evaluating cyclic liquefaction potential using the cone penetration test. *Can. Geotech. J.* 35: 442–459
- [10] Dobry R, Stokoe K H II, Ladd R S, and Youd T L 1981 Liquefaction susceptibility from S-wave velocity. In: *Proc., ASCE Nat. Convention, In Situ Tests to Evaluate Liquefaction Susceptibility, ASCE, New York*
- [11] Stokoe K H, Nazarian S, Rix G J, Sanchez-Salinero I, Sheu J C and Mok Y J 1988 In situ seismic testing of hard-to-sample soils by surface wave method. In: *Earthquake Engineering and Soil Dynamics II—Recent Advances in Ground-motion Evaluation.* ASCE 264–278
- [12] Tokimatsu K and Uchida A 1990 Correlation between liquefaction resistance and shear wave velocity. *Soils Found.* 30: 33–42
- [13] Andrus R D and Stokoe K H II 2000 Liquefaction resistance of soils from shear-wave velocity. *J. Geotech. Geoenviron. Eng.* 126: 1015–1025
- [14] Kayen R, Moss R E S, Thompson E M, Seed R B, Cetin K O, Kiureghian A D, Tanaka Y and Tokimatsu K 2013 Shear-wave velocity–based probabilistic and deterministic assessment of seismic soil liquefaction potential. *J. Geotech. Geoenviron. Eng.* 139: 407–419
- [15] Anbazhagan P, Mog K, Rao K S, Prabhu N S, Agarwal A, Reddy G R, Ghosh S, De M K, Baruah S and Das S K 2019 Reconnaissance report on geotechnical effects and structural damage caused by the 3 January 2017 Tripura earthquake, India. *Nat. Hazards* 98: 425–450
- [16] Ambraseys N N 1988 Engineering seismology: part II. *Earthq. Eng. Struct. Dyn.* 17: 51–105
- [17] Tripura State Pollution Control Board (TSPCB) 2002. <http://trpenvis.nic.in/geog.htm>
- [18] IS 1893, Part 1 2016 Criteria for earthquake resistant design of structures—Part 1: general provisions and buildings. *Bureau of Indian Standards, New Delhi*
- [19] IS 2131, 1981 Method for standard penetration test for soils. *Bureau of Indian Standards, New Delhi*
- [20] ASTM D1586/D1586M-18, 2018 Standard Test Method for Standard Penetration Test (SPT) and Split-Barrel Sampling of Soils. *ASTM International, West Conshohocken, PA*
- [21] Idriss I M and Boulanger R W 2010 SPT-based liquefaction triggering procedures. *Rep. UCD/CGM-10.* 2: 4–13
- [22] Andrus R D, Stokoe K and Hsein Juang C 2004 Guide for shear-wave-based liquefaction potential evaluation. *Earthq. Spectra* 20: 285–308
- [23] Idriss I M 1999 Presentation notes: an update of the Seed-Idriss simplified procedure for evaluating liquefaction potential. In: *TRB Workshop on New Approaches to*

- Liquefaction Anal., Publ. No FHWARD-99-165, Federal Highway Administration, Washington, DC*
- [24] Cetin K O, Seed R B, Der Kiureghian A, Tokimatsu K, Harder L F Jr, Kayen R E and Moss R E 2004 Standard penetration test-based probabilistic and deterministic assessment of seismic soil liquefaction potential. *J. Geotech. Geoenviron. Eng.* 130: 1314–1340
- [25] Iwasaki T, Tokida K I, Tatsuoka F, Watanabe S, Yasuda S and Sato H 1982 Microzonation for soil liquefaction potential using simplified methods. In: *Proceedings of the 3rd international conference on microzonation, Seattle*. 3: 1310–1330
- [26] Luna R and Frost J D 1998 Spatial liquefaction analysis system. *J. Comput. Civil Eng.* 12: 48–56
- [27] Microzonation for Earthquake Risk Mitigation (MERM) 2003. *Microzonation Manual, World Institute for Disaster Risk Management*
- [28] Sonmez H and Gokceoglu C 2005 A liquefaction severity index suggested for engineering practice. *Environ. Geol.* 48: 81–91
- [29] IS 2720, Part 4, 1983 Methods of test for soils: Grain size analysis. *Bureau of Indian Standards (BIS), New Delhi*
- [30] ASTM Committee D-18 on Soil and Rock 2017 Standard Practice for Classification of Soils for Engineering Purposes (Unified Soil Classification System) 1. *ASTM international*
- [31] Tsuchida H 1970 Evaluation of liquefaction potential of sandy deposits and measures against liquefaction induced damage. In: *Proceedings of the Annual Seminar of the Port and Harbour Research Institute*. 3: 3–33
- [32] Building Seismic Safety Council (US), National Earthquake Hazards Reduction Program (US) and BSSC Program on Improved Seismic Safety Provisions 1985. NEHRP (National Earthquake Hazards Reduction Program) Recommended Provisions for the Development of Seismic Regulations for New Buildings: Commentary (Vol. 17). Building Seismic Safety Council, USA
- [33] Seed H B 1987 Design problems in soil liquefaction. *J. Geotech. Eng.* 113(8): 827–845
- [34] Marcuson W F III and Bieganousky W A 1977 SPT and relative density in coarse sands. *J. Geotech. Eng. Div.* 103: 1295–1309

Springer Nature or its licensor (e.g. a society or other partner) holds exclusive rights to this article under a publishing agreement with the author(s) or other rightsholder(s); author self-archiving of the accepted manuscript version of this article is solely governed by the terms of such publishing agreement and applicable law.